APPLIED GEOPHYSICS, Vol.7, No.4 (December 2010), P. 357 - 364, 5 Figures.
DOI: 10.1007/s11770-010-0256-y

Seismic wave propagation in Kelvin visco-elastic VTI media*

Lu Jun[1] and Wang Yun[2]

Abstract: In this article, under the assumption of weak anisotropy and weak attenuation, we present approximate solutions of anisotropic complex velocities and quality-factors for Kelvin visco-elastic transverse isotropy (KEL-VTI) media, based on the complex physical parameter matrix. Also, combined with the KEL-VTI media model, the propagation characteristics of the qP-, qSV-, and qSH-wave phases and energies are discussed. Further, we build a typical KEL-VTI media model of the Huainan coal mine to model the wave propagation. The numerical simulation results show that the PP- and PSV-wave theoretical wave-fields are close to the wave-fields of three-component P- and converted-waves acquired in the work area. This result proves that the KEL-VTI media model gives a good approximation to this typical coalfield seismic-geologic conditions and is helpful to the study of attenuation compensation of multi-component seismic data.
Keywords: KEL-VTI media, complex velocity, quality-factor, anisotropy

Introduction

When seismic waves propagate in the earth, the high frequency components will be strongly absorbed, the seismic waves excited near the surface will show low-frequency (long wavelength) characteristics when propagating at depth. Also, both the seismic field observations and lab studies have demonstrated that most sedimentary rocks display long-wavelength anisotropy, so the anisotropy relates closely with visco-elasticity (Lucet and Zinszner, 1992). Visco-elastic anisotropic media has been researched for many years. Based upon the Kelvin-Voigt constitutive relation, Lamb and Richter (1966) used 21 independent visco-elastic parameters to study the anisotropic attenuation characteristics of quartz crystals. Through petro-physical experiments, Crampin (1981) and Hudson (1982) had observed the Q value anisotropy characteristics of cracked media and arrived at the complex form of the linear viscoelastic Hooke's coefficient. Hosten et al. (1987) determined the attenuation anisotropy characteristics from a composite physical model and found that the attenuation anisotropy is greater than that of velocity in some cases. Zhang et al. (1999) studied the seismic velocity azimuthal anisotropy, attenuation, and quality-factor in extensive dilatancy anisotropic (EDA) media and used the attenuation or Q value of two S-wave types to indicate the presence of cracks. Carcione (1990, 1995) demonstrated that, in visco-elastic anisotropic media (anisotropic

Manuscript received by the Editor June 15, 2009; revised manuscript received November 15, 2010.
*This research is supported by the National 973 Program (Grant No. 2006CB202207) and Special Fund (Grant Nos. 2008ZX05035-001-003, 2008ZX05035-003-004, and 2008ZX05008-006-004).
1. School of Energy Resources, China University of Geosciences, Beijing 100083, China.
2. Institute of Geochemistry, Chinese Academy of Sciences, Guiyang 550002, China.
♦Corresponding author (Wang Yun, Wangyun@mails.gyig.ac.cn).

media with a vertical symmetry axis, also named vertical transversely isotropic or VTI) with the wave propagating vertical to the isotropic plane, there are two dissipation mechanism for P- and S-waves, in other words, each wave has its separate Q value. Zhu and Tsvankin (2006) proposed the attenuation anisotropy equation to express the angular dispersion of the P-, SV-, and SH-wave attenuation coefficients in Thomsen's style of the angular dispersion of velocity in VTI media. These studies show that we cannot correctly understand the propagation of seismic wave-fields unless including a comprehensive consideration of anisotropy and viscoelasticity, which provides a path to enhance the precision of seismic exploration.

In the past ten years, multi-component seismic technology has made great progress but because of the lower dominant frequency of converted shear waves compared with compressional waves, the process of multi-component joint interpretation and inversion has enormous difficulty. There are different characteristics between converted shear and compressional waves reflected from the same geologic body, so it is difficult to carry out horizon correlation and consistently interpret structure. So, it is necessary to research the theories and methods of wave propagation in viscoelastic anisotropic media based on the compensation of converted shear wave attenuation by absorption, restoring its high-frequency components, and enhancing the precision of multi-component seismic surveys (Wang et al., 2009).

For this, we choose the Kelvin transverse isotropic media model with a vertical symmetry axis as the research object to derive a simplified expression and numerical simulation of complex velocity and Q value anisotropy and analyze seismic wave propagation in viscoelastic anisotropic media. This study is very meaningful for recognizing seismic wave attenuation in multi-component seismic surveys and researching more accurate inverse Q compensation methods for complex reservoirs.

Anisotropy of complex velocity and quality-factor

In KEL-VTI media, the stress-strain relationship can be written as:

$$\begin{pmatrix} \sigma_{xx} \\ \sigma_{yy} \\ \sigma_{zz} \\ \sigma_{yz} \\ \sigma_{zx} \\ \sigma_{xy} \end{pmatrix} = \begin{pmatrix} d_{11} & d_{12} & d_{13} & 0 & 0 & 0 \\ d_{21} & d_{22} & d_{23} & 0 & 0 & 0 \\ d_{31} & d_{32} & d_{33} & 0 & 0 & 0 \\ 0 & 0 & 0 & d_{44} & 0 & 0 \\ 0 & 0 & 0 & 0 & d_{55} & 0 \\ 0 & 0 & 0 & 0 & 0 & d_{66} \end{pmatrix} \cdot \begin{pmatrix} \varepsilon_{xx} \\ \varepsilon_{yy} \\ \varepsilon_{zz} \\ \varepsilon_{yz} \\ \varepsilon_{zx} \\ \varepsilon_{xy} \end{pmatrix}, \tag{1}$$

where d_{ij} is the material coefficient of KEL-VTI media, defined as:

$$d_{ij} = c_{ij} - c_{ij}^{'} \frac{\partial}{\partial t} \qquad (i, j = 1,2...6), \tag{2}$$

where c_{ij} are the elastic coefficients of perfectly homogeneous elastic VTI media and c'_{ij} are the viscoelastic coefficients. Equation (2) can be rewritten in the frequency domain as:

$$d_{ij} = c_{ij} + \mathrm{i}\omega c_{ij}^{'} \qquad (i, j = 1,2...6), \tag{3}$$

where ω is the angular frequency. Equations (2) and (3) show that the viscous interaction changes with time and has a linear relationship with frequency.

In anisotropy media, assume X and X' are the elastic and viscous coefficients of the qP-wave (qSV-wave or qSH-wave) in the phase-angle θ direction and $v^2 = X/\rho$ and $v'^2 = X/\rho$. In the time and frequency domains, X and X' have the relationship:

$$X + X^{'} \frac{\partial}{\partial t} \longleftrightarrow X - \mathrm{i}\omega X^{'}, \tag{4}$$

and the analytical expression of complex velocities in KEL-VTI media is:

$$v_{kel-TI}^2 = v^2 - \mathrm{i}\omega v'^2, \tag{5}$$

where v and v' are the elastic- and viscous-phase velocities of seismic wave propagation in viscoelastic media.

In viscoelastic media, quality factor Q is defined as (Carcione, 1990, 1995; Cerveny and Psencik, 2005, 2008):

$$Q = \frac{\mathrm{Re}(v_{kel-TI}^2)}{\mathrm{Im}(v_{kel-TI}^2)} = \frac{v^2}{\omega v'^2}, \tag{6}$$

when Q-1 << 1, substitute equation (6) into equation (5) and take the first-order Taylor approximation to get

$$v_{kel-TI} = \left(v^2 - \mathrm{i}\frac{v^2}{Q} \right)^{\frac{1}{2}} \approx v - \mathrm{i}\frac{v}{2Q}, \tag{7}$$

where the complex velocity real part in KEL-VTI media is the phase velocity in elastic VTI media and the imaginary part indicates the viscoelastic property of the media which can be described by the Q anisotropy. Under the assumption of weak anisotropy (i.e., Thomsen parameters ε, δ, and γ are all far less than 1), the phase-velocity anisotropy versus phase angle θ functions of qP-, qSV-, and qSH-waves in elastic VTI media is given as (Thomsen, 1986):

$$\begin{cases} v_p(\theta) = v_{p0}\left(1+\delta\sin^2\theta\cos^2\theta+\varepsilon\sin^4\theta\right) \\ v_{sv}(\theta) = v_{s0}\left[1+\dfrac{{v_{p0}}^2}{{v_{sv0}}^2}(\varepsilon-\delta)\sin^2\theta\cos^2\theta\right], \\ v_{sh}(\theta) = v_{s0}\left(1+\gamma\sin^2\theta\right) \end{cases} \tag{8}$$

where v_{p0} and v_{s0} are the vertical phase velocities of qP- and qSV- (and qSH-) waves.

Carcione (1990, 1995) and Cerveny and Psencik (2005, 2008) derived and analyzed Q anisotropy but did not give an approximation of the Q function for phase angle. Given the assumption of attenuating VTI media, the symmetry axis is vertical and the attenuation coefficient $A = \gamma/k$ shows the amplitude attenuation rate of each wavelength. The material coefficients c_{ij} are complex and equal to $c_{ij} + i_{c_{ij}}$. Assuming weak anisotropy and weak attenuation, the quality-factor $Q_{ij} = c_{ij}/\ c_{ij}'$ forms a Q matrix (Carcione, 2007):

$$\mathbf{Q} = \begin{pmatrix} Q_{11} & Q_{12} & Q_{13} & 0 & 0 & 0 \\ Q_{12} & Q_{11} & Q_{13} & 0 & 0 & 0 \\ Q_{13} & Q_{13} & Q_{33} & 0 & 0 & 0 \\ 0 & 0 & 0 & Q_{55} & 0 & 0 \\ 0 & 0 & 0 & 0 & Q_{55} & 0 \\ 0 & 0 & 0 & 0 & 0 & Q_{66} \end{pmatrix}. \tag{9}$$

Zhu and Tsvankin (2006) derived the seismic attenuation anisotropy equations:

$$\begin{cases} A_{qP}(\theta) = \dfrac{1}{2Q_{33}}(1+\delta_Q\sin^2\theta\cos^2\theta+\varepsilon_Q\sin^4\theta) \\ A_{qSV}(\theta) = \dfrac{1}{2Q_{55}}(1+\sigma_Q\sin^2\theta\cos^2\theta) \\ A_{qSH}(\theta) = \dfrac{1}{2Q_{55}}(1+\gamma_Q\sin^2\theta) \end{cases} . \tag{10}$$

This equation is similar to the Thomsen velocity anisotropy. $A_p(\theta)$, $Asv(\theta)$, and $A_{sh}(\theta)$ are the attenuation coefficients of qP-, qSV- and qSH-waves at phase angle θ. ε_Q, δ_Q, and γ_Q are the attenuation anisotropy parameters expressed as:

$$\begin{cases} \varepsilon_Q \equiv \dfrac{1/Q_{11}-1/Q_{33}}{1/Q_{33}} = \dfrac{Q_{33}-Q_{11}}{Q_{11}} \\ \gamma_Q \equiv \dfrac{1/Q_{66}-1/Q_{55}}{1/Q_{55}} = \dfrac{Q_{55}-Q_{66}}{Q_{66}} \\ \delta_Q \equiv \dfrac{\dfrac{Q_{33}-Q_{55}}{Q_{55}}c_{55}\dfrac{\left(c_{13}+c_{33}\right)^2}{\left(c_{33}-c_{55}\right)}+2\dfrac{Q_{33}-Q_{13}}{Q_{13}}c_{13}\left(c_{13}+c_{55}\right)}{c_{33}\left(c_{33}-c_{55}\right)} \\ \sigma_Q \equiv \dfrac{\left(1-c_{55}/c_{33}-Q_{33}/Q_{55}\right)\left(\varepsilon-\delta\right)+\left(1-c_{55}/c_{33}\right)\left(\varepsilon_Q-\delta_Q\right)}{\left(c_{55}/c_{33}\right)\left(Q_{33}/Q_{55}\right)} \end{cases} . \tag{11}$$

Equations (9) to (11) are derived based on $C_{ij} = c_{ij} + i_{cij'}$ to get the attenuation parameters and quality-factors, which have no relation with ω, so these equations are not suitable for KEL-VTI media. To solve this problem, we define $d_{ij} = c_{ij} + i\omega c'ij$ for the Kelvin-VTI media. The quality-factor has an inverse relation to frequency and by assuming angular frequency ω is a constant, equation (11) can be derived without considering it. Using $A = \gamma/k= 1/(2Q)$ (Zhu and Tsvankin, 2006), equation (11) can be rewritten in the style suitable for KET-VTI media:

$$\begin{cases} \dfrac{1}{Q_{qP}(\theta)} = \dfrac{f}{Q_{qP0}(f_0)\cdot f_0}(1+\delta_Q(f_0)\sin^2\theta\cos^2\theta \qquad (\quad)\sin\quad) \\ \qquad\qquad\qquad\qquad\qquad\quad +\varepsilon_Q(f_0)\sin^4\theta) \\ \dfrac{1}{Q_{qSV}(\theta)} = \dfrac{f}{Q_{qS0}(f_0)\cdot f_0}(1+\sigma_Q(f_0)\sin^2\theta\cos^2\theta) \\ \dfrac{1}{Q_{qSH}(\theta)} = \dfrac{f}{Q_{qS0}(f_0)\cdot f_0}(1+\gamma_Q(f_0)\sin^2\theta) \end{cases} . \tag{12}$$

where $Q_{qP0}(f_0) = Q_{33}(f_0)$ and $Q_{qS0}(f_0) = Q_{55}(f_0)$ stand for the quality factors of the vertical qP- and qSV- (and qSH-) waves at frequency f_0, respectively. $Q_{qP}(\theta)$, $Q_{qSV}(\theta)$, and $Q_{qSH}(\theta)$ are the quality factors of qP-, qSV-, and *qSH*-waves at frequency f and phase angle θ. $\varepsilon_Q(f_0)$ and $\gamma_Q(f_0)$ are the ratio of the difference between the horizontal and vertical attenuation coefficients to the vertical attenuation coefficient of qP- and qSH-waves at frequency f_0, respectively, i.e., the attenuation anisotropy coefficients of qP- and qSH-waves. $\delta_Q(f_0)$ indicates the relative influence on attenuation between the qP- and qSV-wave quality-factor anisotropies at frequency f_0 in VTI media. $\delta_Q(f_0)$ shows that the quality-factor anisotropy of *qSV*-waves at frequency f_0 is influenced by velocity and attenuation anisotropies simultaneously (Zhu and Tsvankin, 2006).

Seismic wave propagation

Equation (12) gives a clear physical meaning of the complex velocity and quality-factor anisotropy coefficients in KEL-VTI media. When waves propagate in KEL-VTI media, the complex velocity real part stands for the propagation velocity of the seismic constant phase surface, which is the same as the phase velocity in VTI media, and the imaginary part denotes the propagation velocity of the constant amplitude surface. Assume v_{p0} = 3000 m/s, v_{sv0} = 1500 m/s, v_{sh0} = 1500 m/s, ε = 0.2, δ = 0.55, γ = 0.15, f_0 = 20 Hz, $Q_{qP0}(f_0)$ = 30, $Q_{qS0}(f_0)$ = 15, $\varepsilon_Q(f_0)$ = 0.2, $\delta_Q(f_0)$ = 0.55, and $\gamma_Q(f_0)$ = 0.15. From equation (12) we obtain constant phase and amplitude surfaces at different frequencies in KEL-VTI media. The diagrams are shown in Figure 1. In the figure the solid thick coils stand for the constant phase surfaces, and the dashed thin coils stand for the constant amplitude surfaces. From the outer to the inner coils, the frequencies are 15, 20, 25, 30, and 35 Hz, respectively. Apparently, the constant phase surfaces have no dispersion while the constant amplitude surfaces have dispersion. Higher frequencies result in slower constant amplitude surfaces propagation. Even given the same phase velocity and attenuation anisotropy parameters, the constant phase surface and constant amplitude surface shapes are different and the seismic-wave attenuation anisotropy is higher than the velocity anisotropy.

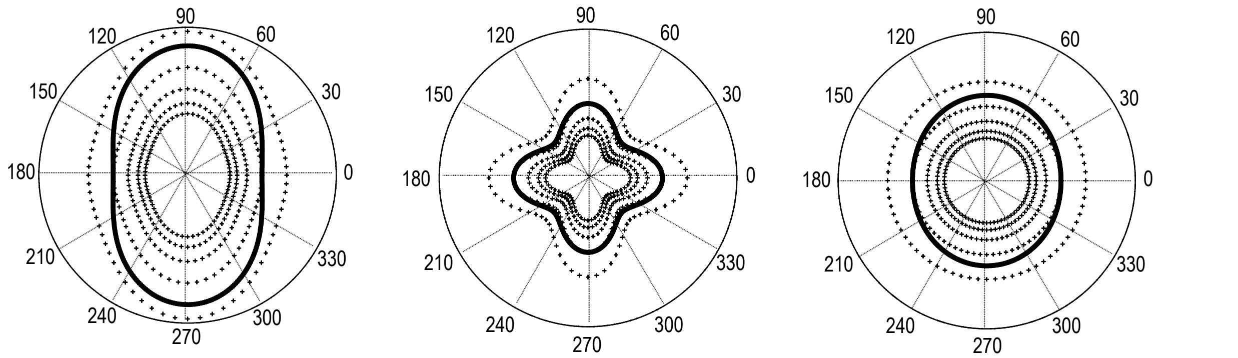

(a) qP-wave (b) qSV-wave (c) qSH-wave

Fig. 1 Plots of constant phase surfaces and constant amplitude surfaces in KEL-VTI media.

(Propagation time is 1 s, the outer circle and labels indicate the phase angle, the outer-circle radiuses of qP- and qSH-waves are 3000 m and 1500 m, respectively.)

Seismic wavelets in KEL-VTI media

Ignoring receiver factors and noise and assuming a loss-free media, the seismic record can be considered as the convolution of the seismic wavelet $w(t)$ and reflection coefficient $r(t)$ (Taner and Coburn,1981)

$$s(t) = w(t) * r(t). \tag{13}$$

The seismic wavelets can be zero-phase, mixed-phase, minimum-phase, and maximum-phase and can be modulated by sine functions of different frequencies with the same initial amplitude (Sheriff, 1995). The equation is given as:

$$w(t) = \int_{f=0}^{\infty} B \cdot \sin(2\pi ft + \phi) df. \tag{14}$$

where B is the initial amplitude, f is the dominant frequency, and ϕ is the initial phase which decides the final stacked wavelet phase. As shown in Figure 2a, the energy of a non-attenuated, zero-phase, seismic wavelet with 10-120 Hz bandwidth is centralized. The propagation of a seismic wavelet stands for the propagation of the wave-train envelope (or group), i.e., the propagation of energy. Compared to the non-attenuated, wide-bandwidth Ricker wavelet in Figure 2b, the waveforms are close to each other. The propagation of some sine wave phase with different frequencies can form the wave front of a seismic wavelet in loss-free media.

Owing to the loss characteristics of KEL-VTI media, dispersion appears in seismic wave propagation and the group velocity and seismic energy propagation velocity are no longer the same, so the convolutional model in loss-free media can’t be applied in KEL-VTI media.

In Kelvin viscoelastic media, the wave number $K = k - i_{\gamma}$, and wave functions have a uniform expression (Niu and Sun, 2007):

$$\mathbf{U} = \mathbf{B} \cdot e^{-\gamma l} \cdot e^{\mathrm{i}(\omega t - kl)}, \tag{15}$$

where $U = (u_1\ u_2\ u_3)^T$ is the matrix of qP-, qSV-, and qSH-wave functions, $B = (B_1\ B_2\ B_3)^T$ is the displacement amplitude matrix of qP-, qSV- and qSH-waves, and l is the propagation distance. Assuming phase angle is θ and substituting $k = 2\pi f / v$ and $\gamma/k = 1/(2Q(\theta))$ into equation (15) gives:

$$\mathbf{U} = \mathbf{B} \cdot e^{-\frac{\pi f}{Q(\theta)}\frac{l(\theta)}{v(\theta)}} \cdot e^{\mathrm{i}(\omega t - kl)}. \tag{16}$$

According to equation (16), the plane wave displacement function solution in KEL-VTI media can be seen as the displacement function solution of plane waves in elastic VTI media with an added amplitude attenuation item: $e^{-\frac{\pi f}{Q(\theta)}\frac{l(\theta)}{v(\theta)}}$.

Since the KEL-VTI media is linear, the superposition principle is applicable, i.e., by Fourier analysis, any vibration can be seen as the superposition of a simple harmonic wave with different frequencies. Using $Q(\theta, f)$ instead of $Q(\theta)$, the seismic wavelet function $w(t)$ in KEL-VTI media can be expressed as:

$$w(t) = \int_{f=0}^{\infty} B \cdot e^{-\frac{\pi ft}{Q(\theta,f)}} \cdot \sin(2\pi ft + \phi) df, \tag{17}$$

where, for zero-phase wavelets, $\phi = -\frac{\pi}{2}$. Ignoring noise and substituting equation (17) into equation (13), we get the convolutional model in the time domain in KEL-VTI media as:

$$s(t) = \int_{f=0}^{\infty} \left(\left(B \cdot e^{-\frac{\pi ft}{Q(\theta,f)}} \cdot \sin(2\pi ft + \phi) \right) * r(t) \right) df. \tag{18}$$

Using equation (18), we can analyze the wavelet form influenced by different quality-factors. Figure 2c shows that when the quality-factor is higher, the wavelet energy is much more centralized, side lobe energy is weak, and the group propagation basically represents the energy propagation. When the quality-factor is low, shown in Figure 2d, the wavelet energy is dispersed, side lobe energy is very strong, the time resolution is small, and the group velocity is no longer consistent with the seismic wave energy propagation velocity.

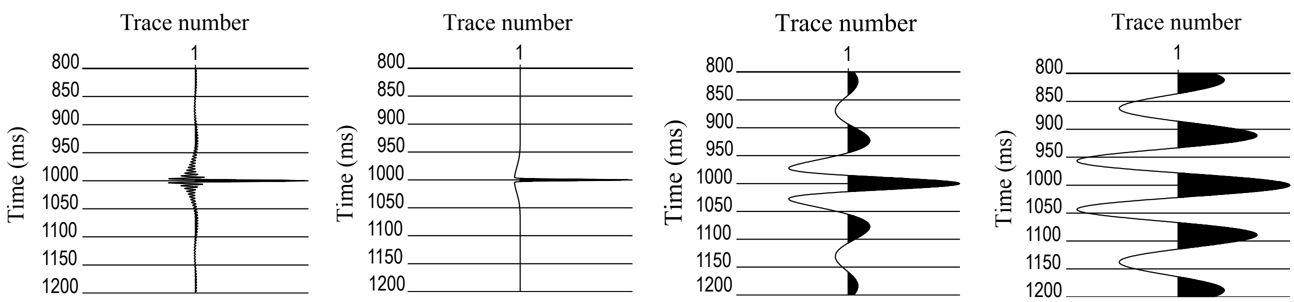

(a) Loss-free wavelet (b) Loss-free Ricker wavelet (c) f_0 = 10 Hz, Q_0 = 120 (d) f_0 = 10 Hz, Q_0 = 15

Fig. 2 Comparison of different zero-phase wavelets (10-120 Hz) with different quality-factors in KEL-VTI media.

Reflection and transmission coefficients of the KEL-VTI model

The complex velocity and wave number in KEL-VTI media are not convenient for expressing the displacement and stress continuity and are also hard to use in seismic modeling. We assume that reflections and transmissions at the KEL-VTI media interface are instantaneous like in the elastic VTI media and viscosity is taken into effect when new disturbances begin, which is exhibited by wavelet attenuation during propagation. So, before AVO analysis, an exponential function is often used to compensate for the viscoelastic absorption in the seismic wave propagation to derive true reflection coefficients.

The expressions of equations (17) and (14) are the same assuming $A = B \cdot e^{-\frac{\pi ft}{Q(\theta,f)}}$, and then the form of the seismic wave potential function in KEL-VTI media is the same as in elastic media. This is convenient to calculate reflection and transmission coefficients using the quasi-elastic method. Banik (1987) gave its expressions.

Using A_2/A_1 to express the reflection (or transmission) coefficient at the interface,

$$\frac{A_2}{A_1} = \frac{B_2}{B_1} \cdot e^{-\pi f\left(\frac{t_2}{Q_2(\theta_2,f)} - \frac{t_1}{Q_1(\theta_1,f)}\right)}, \tag{19}$$

where the mutual conversion of phase angles θ_1 and θ_2 satisfies the Snell law. Therefore, if assuming the wavelet has no attenuation, the reflection (or transmission) coefficient of the KEL-VTI media is the function of time (equation (19)). We can use the attenuation-free seismic wavelet function to convolve the time-varing elastic reflection (or transmission) coefficient function. Contrarily, we can use the time-varing attentuated wavelet to convolve the elastic reflection coefficient function.

Wave-field characteristics in real KEL-VTI media

The theories and methods researched in this paper are introduced into practice of the 3D-3C seismic exploration area in the Guqiao coal mine in the Huainan area.

In the study area, the shallow layer is an unconsolidated layer more 500 m in thickness containing clays and drift sand. The coal layer is a typical sand, mud, carbon-based, thin, interbedded layer, which is a type of KEL-VTI media (Wang et al, 2009). The parameters of this model are given in Table 1. The ray tracing method is used to perform seismic modeling in both elastic and viscoelastic media regardless of spherical diffusion. The source frequency bandwidth is 10-120 Hz. For analytical convenience, PP-waves are only recorded by the Z component and SV-waves by the X component. The modeled results are shown in Figures 3 and 4. From Figure 3 we see that the elastic VTI media seismic wave amplitude has no attenuation, the frequency band is wide, and the time resolution is high. We can identify the coal seam roof and floor easily. The coal seam roof reflection is negative and the coal seam floor reflection is positive. The spectral difference over offset can indicate the AVO effect. PSV-wave amplitude is stronger in the middle offsets, while the PP-wave is stronger at near offsets.

In Figure 4, we see that the time resolution of the PP- and PSV-waves is worse. The coal seam roof and floor cannot be identified in the complex reflected waves. The PP-wave frequency band is wider than the PSV-wave, with the upper cutoff-frequency of 100 Hz and the dominant frequency is from 10 to 80 Hz. For the PSV-wave, the upper cutoff -frequency is 60 Hz and the dominant frequency is in the range of 10 to 40 Hz. The PP-wave maximum amplitude is at near offsets, while the PSV-wave maximum is at 700 m offset. That is because of the comprehensive influences of AVO and quality factor anisotropy.

The Z and X components of a field three-component shot record (after compensation of spherical diffusion) are shown in Figure 5. The amplitude near the surface is much stronger than deeper. The red box indicates the reflection from the coal seam and we see that the upper frequency limit and dominant frequency of the real data are close to the modeled result. We conclude that the KEL-VTI model matches the real coal reflections than does the elastic VTI model and describes the velocity and quality-factor anisotropy more accurately.

Table 1 P- and S-wave velocity and anisotropic quality factor

Layers No.	Lithology	Depth of bottom interface(m)	v_{qP0} (m / s)	v_{qS0} (m / s)	ρ (g / cm^3)	ε	δ	Q_{qP0} (30Hz)	Q_{qS0} (15Hz)	ε_Q	δ_Q
1	Sand-shale	700	2280	1486	2.35	0.12	0.084	86	47.5	-0.2	0.13
2	13-1 coal	705	2050	1355	1.5	0.008	0.046			-0.15	0.056
3	Sand-shale	775	3300	2064	2.4	0.106	0.06			-0.05	0.11
4	11-2 coal	778	2100	1383	1.52	0.002	0.001			0	0
5	Sand-shale	858	3400	2121	2.5	0.005	0.003			-0.001	0.001
6	8 coal	861	2150	1412	1.55	0	0	77	29.7	-0.002	0.003
7	Sand-shale	901	3500	2177	2.6	0.052	0.076			0.001	0.006
8	6 coal	904	2200	1440	1.58	0	0			0	0
9	Sand-shale	1014	3600	2234	2.65	0.068	0.07			0.006	0.008
10	1 coal	1021	2300	1497	1.6	0.004	0.001			-0.006	0.007
11	Sand-shale	2000	4000	2461	2.7	0	0	250	150	0	0

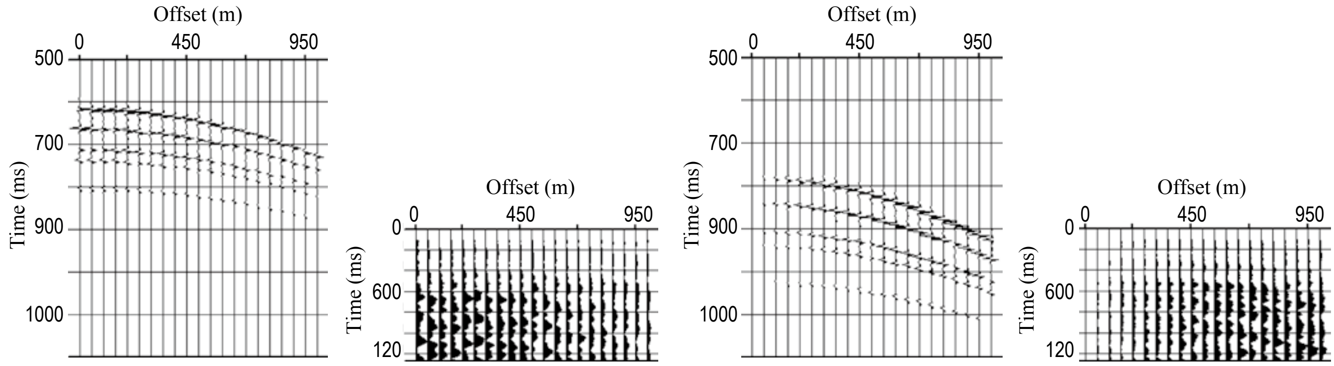

(a) PP-wave (b) PP-wave spectrum (c) PSV-wave (d)PSV spectrum

Fig. 3 Reflected waves of the elastic VTI media and their corresponding spectrum.
(Frequency band: 10-120 Hz)

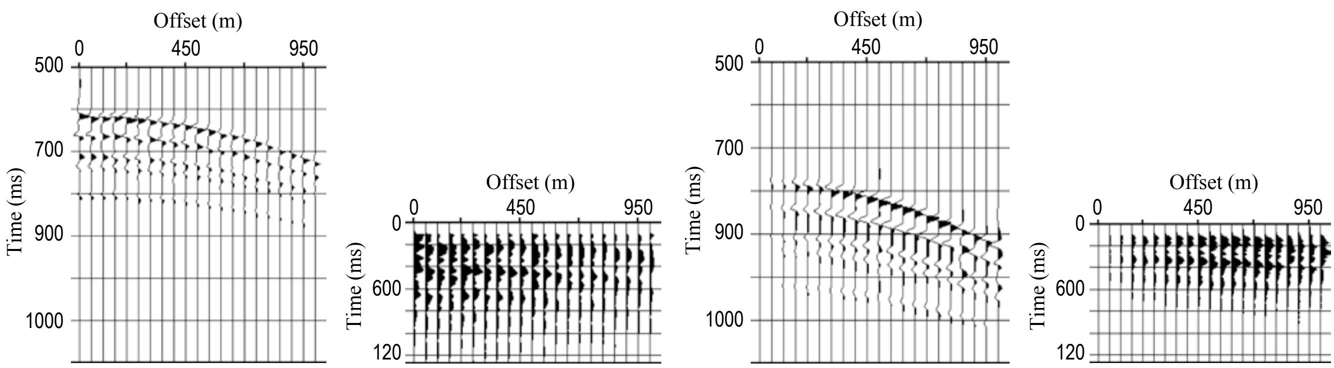

(a) PP-wave (b) PP-wave spectrum (c) PSV-wave (d)PSV spectrum

Fig. 4 Reflected waves of KET-VTI media and their corresponding spectrum.
(Frequency band: 10-120Hz)

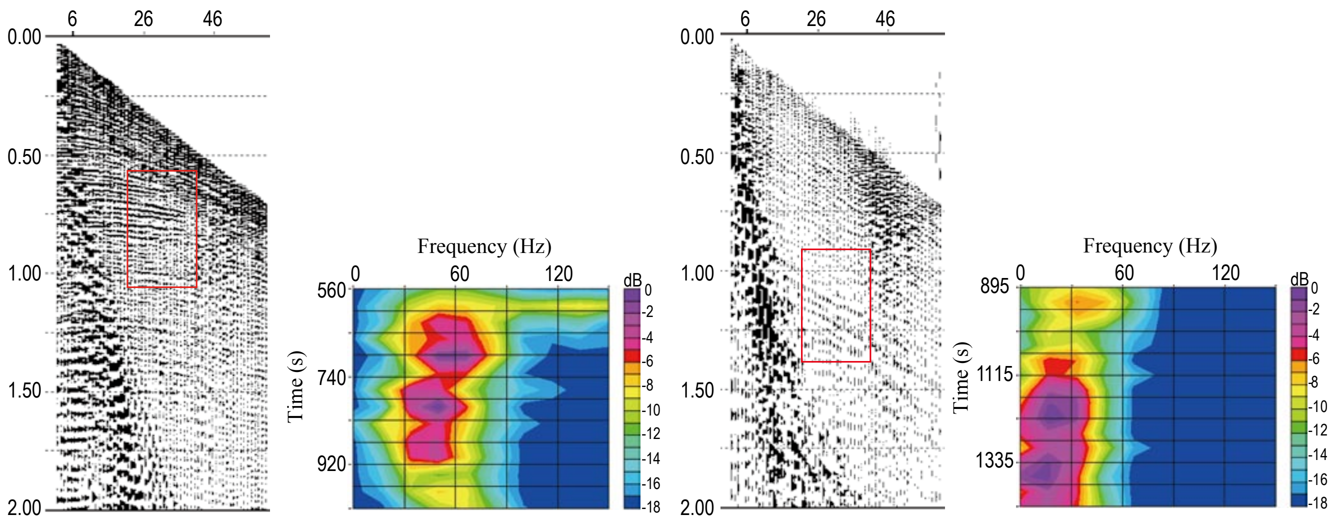

(a) Z-component (b) Z-component spectrum (c) X-component (d) X-component spectrum.

Fig. 5 A single shot of real data and the corresponding reflected wave spectrum.
(Reflection in the red box is the coal layer)

Conclusions

The seismic wave-field simulation in KEL-VTI media showed that, because of visco-elasticity and anisotropy, the high frequency part of seismic wavelet is attenuated intensively and the wavelet envelope was more divergent, which agrees with the wave-field characteristics recorded in multi-component seismic exploration. At present, based on the isotropy and frequency independent assumptions, Q estimation and inverse Q compensation methods are hardly satisfactory in multi-component seismic processing. The comparison of the simulated classical KFL-VTI media wave-field and the practical wave-field in the Huainan Guqiao coal mine illustrates that the KEL-VTI assumption is closer to the real coal measure strata and could better explain the rules of seismic propagation and attenuation in VTI layers, It also provides a theoretical basis for exploring more precise anisotropic Q compensation for multi-component seismic data.

References

Banik, N. C., 1987, An effective anisotropy parameter in transversely isotropic media: Geophysics, 52 (12), 1654 – 1664.

Carcione, J. M., 1990, Wave propagation in anisotropic linear viscoelastic media: Theory and simulated wavefield: Geophys. J. Int., **101**, 739 – 750.

Carcione, J. M., 1995, Constitutive model and wave equations for linear, viscoelastic, anisotropic media: Geophysics, **60**(2), 537 – 548.

Carcione, J. M., 2007, Wave fields in real media: Wave propagation in anisotropic, anelastic, porous and electromagnetic media: 2nd Ed., Elsevier Science.

Cerveny, V., and Psencik, I., 2005, Plane waves in viscoelastic anisotropic media - I: Theory: Geophys. J. Int., **161**(1), 197 – 212.

Cerveny, V., and Psencik, I., 2008, Quality factor Q in dissipative anisotropic media: Geophysics, **73**(4), T63 – T75.

Crampin, S., 1981, A review of wave motion in anisotropic and cracked elastic –media: Wave Motion, **3**, 343 – 391.

Hosten, B., Deschamps, M., and Tittmann, B. R., 1987, Inhomogeneous wave generation and propagating in lossy anisotropic solids: Application to the characterization of viscoelastic composite materials: J. Acoust. Soc. Am., **82**, 1763 – 1770.

Hudson, J. A., 1982, Over all properties of a cracked solid: Math. Proc. Camb. Phil. Soc., **88**, 371 – 384.

Lamb, J., and Richter, J., 1966, Anisotropic acoustic attenuation with new measurements for quartz at room temperature: Proc. Roy. Soc. London, Ser. A, **293**, 479 – 492.

Lu, J., Wang, Y., and Shi, Y., 2006, The best receiving window for acquisition of multicomponent converted seismic data in VTI media: Chinese J. Geophys. (in Chinese), **49**(1), 234 – 243.

Lucet, N., and Zinszner, B., 1992, Effects of heterogeneities and anisotropy on sonic and ultrasonic attenuation in rocks: Geophysics, **57**(8), 1018 – 1026.

Niu, B. H., and Sun, C. Y., 2007, Viscoelastic medium and seismic wave propagation, half-space homogeneous isotropic: Geological Publishing House, Beijing.

Sheriff, R. E., 1995, Exploration seismology (second edition): Cambridge University Press, 181 – 183.

Taner, M. T., and Coburn, K., 1981, Surface-consistent deconvolution: 51st Ann. Internat. Mtg., Soc. Expl. Geophys.

Thomsen, L., 1986, Weak elastic anisotropy: Geophysics, **51**, 1954 – 1966.

Wang, Y., Lu, J., and Shi, Y., et.al, 2009, PS-wave Q estimation based on the P-wave Q values: J. Geophys. Eng., **6**, 386 – 389.

Zhang, Z. J., Teng, J. W., and He, Z. H., 1999, The study of seismic wave azimuthal anisotropic character of velocity attenuation, and quality factor in EDA media: Science China (E edition), **29**(6), 569 – 574.

Zhu, Y., and Tsvankin, I., 2006, Plane-wave propagation in attenuative transversely isotropic media: Geophysics, **71**(2), T17 – T30.

Lu Jun: See biography and photo in the Applied Geophysics March 2010 issue, P. 97.